The 9th European Congress on Computational Methods in Applied Sciences and Engineering
ECCOMAS Congress 2024
3–7 June 2024, Lisboa, Portugal

# PERFORMANCE AND STABILITY ASSESSMENT OF A COUPLED THREE-FIELD THERMAL FLUID-STRUCTURE INTERACTION SIMULATION OF A SIMPLIFIED THIN-WALLED SKIN HEAT EXCHANGER

**Lasse Kreuzeberg[1,2], Matthias Haupt[1,2], Daniel Hahn[1,2], Ihar Antonau[1,3] and Sebastian Heimbs[1,2]**

[1] Cluster of Excellence SE$^2$A - Sustainable and Energy-Efficient Aviation
Technische Universität Braunschweig
Hermann-Blenk-Str. 42, 38108 Braunschweig, Germany
e-mail: se2a@tu-braunschweig.de, www.tu-braunschweig.de/en/se2a

[2] Institute of Aircraft Design and Lightweight Structures (IFL)
Technische Universität Braunschweig
Hermann-Blenk-Str. 35, 38108 Braunschweig, Germany
email: ifl@tu-braunschweig.de, www.tu-braunschweig.de/en/ifl

[3] Institute of Structural Analysis (ISD)
Technische Universität Braunschweig
Beethovenstr. 51, 38106 Braunschweig, Germany
email: isd@tu-braunschweig.de, www.tu-braunschweig.de/en/isd

**Key words:** Performance Analysis, Stability Assessment, Coupled Thermal Fluid Structure Interaction, Numerical Simulation, Heat Transfer

**Summary.** This paper presents a performance and stability assessment of a two-dimensional, three-field conjugate heat transfer problem encompassing an aerodynamic flow domain, a thin solid domain, and a cooling fluid channel. The study focuses on the chosen coupling relaxation methods and boundary conditions at the coupling interfaces.

Both fluid domains are modeled using Navier-Stokes equations for compressible fluids, while the solid domain employs heat transfer equations akin to those for aluminium. The coupling procedure adopts a Dirichlet-Neumann approach, enabling heat flux and temperature exchanges between domains. To enhance system stability, especially in pure Neumann boundary condition scenarios, the coupling is executed using a pseudo-transient approach. This strategy allows transient solutions for the solid domain and stationary convergence for the fluid domains.

Coupling relaxation methods are applied to stabilise the convergence process. Factors impacting performance and stability are analysed by adjusting selected coupling parameters while keeping solver parameters constant. The study underscores the importance of relaxation methods in addressing overestimated interface values during partitioned coupling, thereby improving the coupling convergence rate.

This assessment provides insights into optimising the coupling strategies for thin-walled conjugate heat transfer problems under multi-physical interactions, revealing critical dynamics that ensure computational efficiency and system stability.

## 1 INTRODUCTION

The Cluster of Excellence SE²A - Sustainable and Energy Efficient Aviation at the Technische Universität Braunschweig is proposing new concepts and solutions for green aviation. One of its projects deals with the development of skin heat exchangers for unconventional aircraft configurations, such as the blended wing body, which are used to dissipate the waste heat generated by the fuel cells that power the aircraft.

For future research a coupling framework will be developed that can couple different solvers in a partitioned approach, which are optimised for their respective domain of application. In addition to coupling the three domains (aerodynamic flow, structure and cooling fluid flow), the framework will be able to optimise heat exchanger size, position, cooling channel layout and geometry. The aim is to provide a coupling framework capable of designing such skin heat exchangers for given geometries and flight missions.

A coupled simulation of such complexity, including the overall aerodynamics of the aircraft with thermal and mechanical structural behaviour, the relatively small cooling ducts and the optimisation of all disciplines, is not feasible even with the computing power currently available in a reasonable amount of time. Therefore, investigating every small detail of the simulation process for performance improvement can be beneficial to the overall performance of the subsequent expensive simulations. Since the individual solver time is estimated to be the most computationally expensive part of the simulation, one of the crucial things to investigate is the reduction of coupling iterations.

In this work a simple two-dimensional case derived from [1] is set up. The three-field conjugate heat transfer problem consists of two fluid domains and a thin-walled solid domain in between. The whole system is modelled in a partitioned approach using separate cases in OpenFOAM® v2012 [2].

The focus is on the coupling relaxation schemes, which are applied to the interface vectors exchanged between adjacent domains. The coupling relaxation schemes used are a constant relaxation factor, the Aitken method for coupled systems [3] and a multi-vector quasi-newton method proposed by Bogaers [4]. All these relaxation methods have already been implemented in the coupling framework.

In addition, after the relaxation method is evaluated, the coupling algorithm between two domains is reversed, i.e. instead of the conventional Dirichlet-Neumann approach or flux forward/temperature back (FFTB) algorithm, a Neumann-Dirichlet approach or temperature forward/flux back (TFFB) algorithm is used [5].

## 2 IMPLEMENTATION

When coupling three different solvers to each other, their communication needs to be clearly defined and set up before the actual computation starts. The communication definition includes the determination of quantities that are exchanged, the mapping method used for adjacent domains, the boundary conditions that are applied to the individual solver domains, the coupling convergence criteria and coupling sequence.

In the introduced project the open source framework KratosMultiphysics and its included CoSimulationApplication [7] (CoSim in the following) is used as the coupling framework. CoSim already includes several mapping types, convergence accelerators and convergence criteria definitions. Also, the communication is fully defined and is ready to use. Given this, there are only

a few settings such as the coupling sequence and specification of external solvers that need to be adjusted.

CoSim uses a well-defined internal MappingApplication that takes care of appropriate quantity mapping between the solver domains. Apart from conform meshes it can also handle non-conform meshes. However, for the sake of simplicity and to reduce mapping overhead, conform meshes are used in the present work.

When using CoSim any black-box solver that can be controlled remotely and provides access to its models interface data can be used. All that needs to be done is the development of a SolverWrapper, which connects the input-output (IO) interface of the black-box solver or software to the one provided by CoSim (see figure 1). In this SolverWrapper various functions need to be implemented for CoSim to know what to do when certain functions are called. The internal sequence of each individual solver is fully defined and only the coupling sequence needs to be specified.

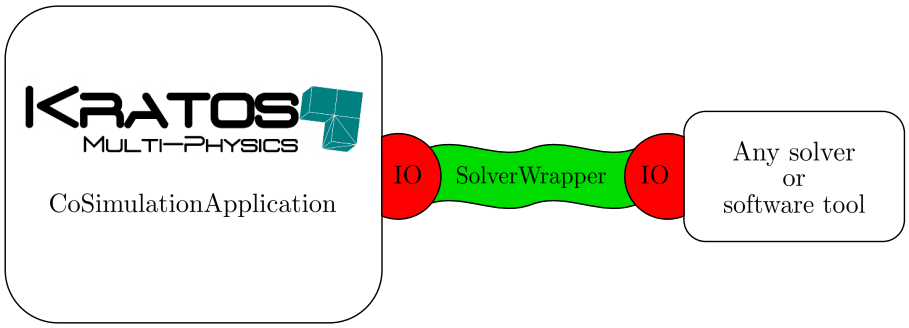


**Figure 1**: Solver implementation in KratosMultiphysics' CoSimulationApplication

## 3 NUMERICAL METHODS

### 3.1 Geometry and mesh

The overall geometry, which is derived from Birken [1], consists of three domains, from top to bottom namely the aerodynamic flow, a thin flat plate and the cooling fluid channel, respectively (see figure 2). All domains are connected via their coupling interfaces $\Gamma_{air-solid}$ and $\Gamma_{water-solid}$ and discretised using a Cartesian grid.

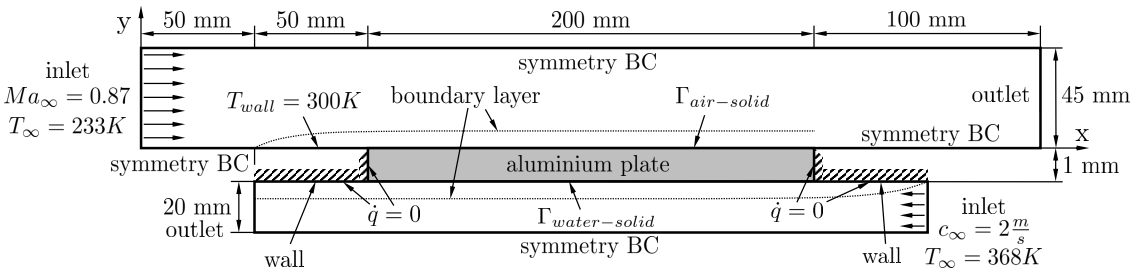


**Figure 2**: Scheme of the used two dimensional case setup

The aerodynamic flow domain contains four sections. All four sections have a symmetry boundary condition at the top side and a geometrical height of 45 mm. A uniform fixed value inlet condition, where the air flow enters the domain is applied at $x = 0\,\text{mm}$.

On the bottom side several different boundary conditions are imposed. The first 50 mm with a symmetry boundary condition are followed by a 50 mm long heated wall that enforces a no-slip boundary condition and helps developing a proper boundary layer upstream of the coupling interface. At $x = 100\,\text{mm}$ the coupling interface starts with a length of 200 mm. The last section is a 100 mm symmetry boundary condition, which ends with the flow outlet at $x = 400\,\text{mm}$.

The mesh consists of $18,240$ cells, with 96 cells in y-direction. The first and last sections each have 20 equally distributed cells in x-direction. In the second section of the domain are 30 cells in x-direction with a constant mesh expansion ratio of $\delta_e/\delta_s = 0.3$ towards the coupling interface. The coupling interface itself is constructed of 120 equally distributed boundary faces. All four sections have the same constant mesh expansion ratio in the y-direction, which results in the smallest cell right next to the coupling interface having a height of $\delta_b = 2.4 \cdot 10^{-3}\,\text{mm}$.

The solid domain has a height of 1 mm to approach a thin-walled aircraft skin. The top and bottom sides are the two coupling interfaces $\Gamma_{air-solid}$ and $\Gamma_{water-solid}$ towards the aerodynamic flow and the cooling channel, respectively. The boundary conditions of the left and right side are idealised as adiabatic. The domain has a total cell count of $2,520$ cells with 120 cells in x-direction and 21 cells in y-direction. All cells have the same size and are equally distributed over the domain.

The cooling channel domain consists of three sections with a height of 20 mm. The flow enters at the right side at $x = 350\,\text{mm}$ and leaves the domain at $x = 50\,\text{mm}$. The bottom side of the domain is governed by a symmetry boundary condition. As in the aerodynamic domain, there is a no-slip boundary condition upstream of the coupling interface. Additionally, to resemble a cooling channel, there is also a no-slip boundary condition applied downstream of the coupling interface. Both peripheral walls are considered adiabatic.

This domain is discretised into $9,000$ cells. All sections have 50 cells in the y-direction, which are imposed by a constant mesh expansion. The smallest cell right next to the coupling interface has a height of $2.06 \cdot 10^{-3}\,\text{mm}$. The domain section that includes the coupling interface has 120 cells in x-direction, the other two sections each have 30 cells in x-direction. In the x-direction no mesh expansion is applied. The selected grid sizes at the coupling boundaries result in $y^+$ values of approximately $y^+ \approx 0.25$ for both fluid domains, thereby ensuring an adequate level of accuracy of the thermal quantities exchanged.

### 3.2 Boundary conditions and initialisation

The boundary conditions are chosen to be in a realistic range to resemble the expensive future simulations. However, to reduce computational cost of this simple case, both fluid cases are considered laminar. As the initially introduced aircraft is estimated to have a cruise altitude of around $8,000\,\text{m}$, the air temperature can be approximated at $233\,\text{K}$. With a Mach number of $Ma_\infty = 0.87$ on the wing, the resulting velocity is around $c = 265\,\frac{\text{m}}{s}$. The spatially and temporally constant wall temperature of the upstream wall is $T_{wall} = 300\,\text{K}$.

For the cooling fluid channel, the temperature is estimated to be $T_{cool} = 368\,\text{K}$ with a velocity of $c_{cool} = 2\,\frac{\text{m}}{\text{s}}$ in the negative x-direction. The walls upstream and downstream of the coupling interface enforce a no-slip condition on the velocity field and a zero-gradient condition on the

temperature field.

For both fluid domains the coupling interface acts like a no-slip wall. In the baseline case, Dirichlet (temperature) boundary conditions are applied to the fluid domains and Neumann (heat flux) boundary conditions to the solid domain (FFTB). Later this coupling implementation is varied. The outlet boundary condition for both aerodynamic flow and cooling channel is a zero-gradient condition for both energy and momentum.

The initial spatially constant temperature of the solid domain is initialised with $T_{init} = 300\,\mathrm{K}$.

### 3.3 Governing equations and material properties

Both fluid domains are governed by the Navier-Stokes equations for compressible fluids (see equations (1) to (3)), which are implemented in the solver rhoSimpleFoam of OpenFOAM® v2012. As the fluid flows are computed in a stationary manner, the unsteady terms are not considered. A detailed derivation of the Navier-Stokes equations can be found in e.g. [6]. The used symbols are described in table 1.

$$\nabla \cdot (\rho \mathbf{v}) = 0 \tag{1}$$

$$\nabla \cdot (\rho \mathbf{v}\mathbf{v}) = -\nabla p + \mu \nabla^2 \mathbf{v} + \mathbf{f}_b \tag{2}$$

$$\nabla \cdot (\rho \mathbf{v} e) = -\nabla \cdot \dot{q}_s - \nabla(p\mathbf{v}) + \nabla \cdot (\boldsymbol{\tau} \cdot \mathbf{v}) + \mathbf{f}_b \cdot \mathbf{v} + \dot{q}_V \tag{3}$$

**Table 1**: Variables in the Navier-Stokes equations

| symbol | meaning |
|---|---|
| $\nabla$ | nabla operator |
| $\rho$ | density |
| $\mathbf{v}$ | velocity vector |
| $p$ | pressure |
| $\mu$ | dynamic viscosity |
| $\mathbf{f}_b$ | body forces vector |
| $e$ | specific total energy |
| $\boldsymbol{\tau}$ | stress tensor |
| $\dot{q}_S$ | rate of heat transfer across surfaces |
| $\dot{q}_V$ | rate of heat source or sink |

For the sake of simplicity, the present modelled fluids are chosen to be air and water. However, non of the material characteristics remain constant in the respective domain and are approximated using polynomials that were derived from [8]. For the aerodynamic domain the viscosity $\mu$ is modelled using the transformed Sutherland law [9] (see equation (4)).

$$\mu = A_s \frac{\sqrt{T}}{1 + T_S/T} \tag{4}$$

with the model coefficients for air

$$A_s = 1.46 \cdot 10^{-6}$$
$$T_S = 110.4\,\mathrm{K}$$

and temperature $T$.

The solid domain is solved using the solver solidFoam of OpenFOAM® v2012. The temperature distribution in the domain is solved by solidFoam using equation (5).

$$\rho c_p \frac{\partial T}{\partial t} = \lambda \nabla^2 T + \dot{q}_V \tag{5}$$

where $\rho$ is the density of the solid domain, $c_p$ the specific heat capacity and $\lambda$ the heat conductivity. $T$ is the temperature and $\dot{q}_V$ the heat fluxes that are applied to the finite volumes. The material characteristics of the solid domain are similar to the ones of aluminium (see table 2) and approximated being constant and isotropic.

**Table 2**: Material properties for the solid domain

| property | value | unit |
|---|---|---|
| density $\rho$ | 2,700 | $\mathrm{kg/m^3}$ |
| specific heat capacity $c_p$ | 837 | $\mathrm{J/(kg \cdot K)}$ |
| heat conductivity $\lambda$ | 236 | $\mathrm{W/(m \cdot K)}$ |

### 3.4 Coupling procedure

To define the coupling procedure each domain has to be specified in terms of the applied boundary conditions at their coupling interface. Thermal coupling takes place with a Dirichlet-Neumann or Neumann-Dirichlet approach. Thus, heat fluxes and temperatures at the coupling interfaces are exchanged. A typical approach is to use the FFTB scheme [5], in which the heat fluxes are applied to the domain that possesses higher heat conductivity. Applying that approach to both coupling interfaces, the solid domain becomes a Neumann-Neumann problem since the heat fluxes are applied at both coupling interfaces $\Gamma$. With the side walls set as zero-gradient boundary conditions, the domain problem is defined by Neumann boundary conditions only.

A pure Neumann problem without any Dirichlet or Robin boundary conditions is challenging to model in a stationary manner. This is due to the fact that a stationary solution does not exist if the net heat flux of the domain is not equal to zero. Treating all individual cases in a stationary manner is therefore likely to result in divergence of the solid domain in terms of the temperature distribution.

In order to achieve some sort of a natural damping of the imposed heat fluxes, the domains are coupled using a pseudo-transient approach. This approach involves solving the solid domain in a transient manner, while the fluid domains converge to a stationary solution for each iteration. As a result, the heat fluxes are only applied for a limited amount of time, which results in a more stable coupled system.

During the computation of the solid domain, the boundary conditions are applied temporally constant, starting with an initial heat flux of $\mathbf{q}^{i=0}_{\Gamma_j,k=0} = 0$ for the first iteration $i$ in time step $k$ and at interface $j$. After that, the resulting temperatures $\mathbf{T}^0_{\Gamma_j,0}$ at the interfaces are sent to the respective fluid domains $\Omega_j$, which return the new heat fluxes $\mathbf{q}^1_{\Gamma_j,0}$ that result after convergence.

Additionally a coupling relaxation scheme is applied to the temperature vectors $\mathbf{T}^i_{\Gamma_j,k}$ that are sent to the fluid domains. To monitor the coupling residual in every iteration, these vectors are stored and compared to each other. As soon as changes of these vectors in between two iterations are smaller than the coupling criteria of $\epsilon_c < 5 \cdot 10^{-5}$, the time step converges and the next time step is started with the obtained temperature fields of the individual domains.

### 3.5 Used relaxation methods

In this study the impact of the coupling parameters is investigated. Therefore, the individual solver parameters are not changed during this parameter study. However, some coupling parameters are adjusted to investigate the individual impact on performance and stability.

During partitioned coupling the interface values are often overestimated. To stabilise and thus speed up the coupling convergence, relaxation methods are used to relax the exchanged fields. In this section the used relaxation methods are addressed briefly.

When the temperature interface vectors are relaxed, the new temperature vector $\mathbf{T}^i_{\Gamma,k}$ is calculated as a mixture between the temperature field of the last iteration $\mathbf{T}^{i-1}_{\Gamma,k}$ and the new unrelaxed temperature field $\widetilde{\mathbf{T}}^i_{\Gamma,k}$ according to equation (6).

$$\mathbf{T}^i_{\Gamma,k} = \mathbf{T}^{i-1}_{\Gamma,k} \cdot (1 - \omega^i) + \widetilde{\mathbf{T}}^i_{\Gamma,k} \cdot \omega^i \tag{6}$$

In this study three methods have been used for relaxation. The constant and Aitken methods both calculate the relaxation factor $\omega^i$ for the next coupling iteration. The third method is a multi-vector quasi-newton method (MVQN in the following) that uses a system Jacobian to calculate the relaxed temperature field.

The constant relaxation scheme is straightforward and uses a predefined relaxation factor that remains constant at all times (see equation (7)).

$$\omega^i = \omega^{i-1} = const \tag{7}$$

The Aitken method for coupled systems [3] calculates the new relaxation factor while considering the change of the interface temperature of the last two iterations. For that, some computational inexpensive calculations are required (see equation (8)).

$$\omega^i = \omega^{i-1} \cdot \frac{(\mathbf{r}^{i-1})^T(\mathbf{r}^i - \mathbf{r}^{i-1})}{(\mathbf{r}^i - \mathbf{r}^{i-1})^2} \tag{8}$$

with $\mathbf{r}^i$ being the residual of the current, still unrelaxed, temperature vector and the one before

$$\mathbf{r}^i = \widetilde{\mathbf{T}}^i_\Gamma - \mathbf{T}^{i-1}_\Gamma. \tag{9}$$

For the previous iteration the already relaxed temperature vectors are taken into account.

The MVQN method [4], similar to the Broyden method, constructs an approximated Jacobian matrix that transforms the residuals of the temperature vector to the changes of the heat flux vectors. Unlike the Broyden method, the MVQN method does not only consider the previous iterations of the same time step, but can also take previous time steps into account by iteratively updating its Jacobian matrix. A disadvantage of this method is that it requires to store matrices and that its overhead is bigger than e.g. the Aitken method because of more

expensive computational operations. However, it was shown that this method can reduce the number of coupling iterations, which has a favourable effect on the overall performance [4].

To approximate the system Jacobian matrix, two observation matrices, which include the residuals of the last iterations, are constructed using

$$\Delta\mathbf{T}_{\Gamma_j,k} = [\mathbf{T}^{i}_{\Gamma_j,k} - \mathbf{T}^{i-1}_{\Gamma_j,k}, \mathbf{T}^{i-1}_{\Gamma_j,k} - \mathbf{T}^{i-2}_{\Gamma_j,k}, ..., \mathbf{T}^{2}_{\Gamma_j,k} - \mathbf{T}^{1}_{\Gamma_j,k}] \tag{10}$$

$$\Delta\mathbf{Q}_{\Gamma_j,k} = [\mathbf{q}^{i}_{\Gamma_j,k} - \mathbf{q}^{i-1}_{\Gamma_j,k}, \mathbf{q}^{i-1}_{\Gamma_j,k} - \mathbf{q}^{i-2}_{\Gamma_j,k}, ..., \mathbf{q}^{2}_{\Gamma_j,k} - \mathbf{q}^{1}_{\Gamma_j,k}] \tag{11}$$

where the matrix $\Delta\mathbf{Q}_{\Gamma_j,k}$ stores the heat fluxes of coupling interface $j$ of the last $i$ iterations of time step $k$. Now an approximated Jacobian matrix can be constructed that relates the changes of the temperature vectors to the changes of the heat flux vectors of the current time step.

$$\mathbf{J}_{\Gamma_j,k} \;\Delta\mathbf{T}_{\Gamma_j,k} = \Delta\mathbf{Q}_{\Gamma_j,k} \tag{12}$$

After each coupling iteration, the Jacobian matrix gets updated with respect to a specific updating rule (see equation (13)). This equation also requires the old Jacobian matrix $\mathbf{J}_{\Gamma_j,k-1}$ to include information about the previous time step.

$$\mathbf{J}_{\Gamma_j,k} = \mathbf{J}_{\Gamma_j,k-1} + \left(\Delta\mathbf{Q}_k - \mathbf{J}_{\Gamma_j,k-1}\,\Delta\mathbf{T}_{\Gamma,k}\right)\left(\left(\Delta\mathbf{T}_k\right)^T\Delta\mathbf{T}_k\right)^{-1}\left(\Delta\mathbf{T}_k\right)^T \tag{13}$$

To provide a Jacobian matrix in the very first iteration, the initial Jacobian matrix is defined as $\mathbf{J}_0^0 = [\mathbf{0}]$. Because the MVQN method requires at least two coupling iterations, the first two iterations are relaxed using the constant method mentioned before.

## 4 RESULTS

In all cases, the simulation results obtained after six seconds of simulation time are identical (see figure 3). This outcome is to be expected, given that only the coupling procedure was modified.

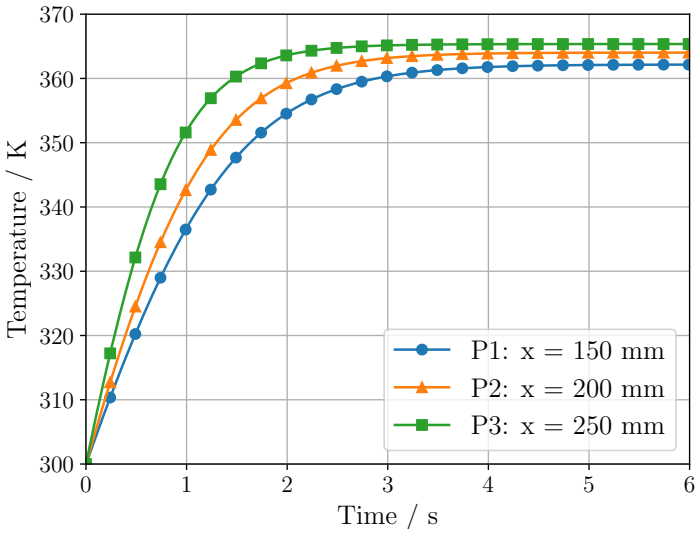


**Figure 3**: Transient temperature trend for three different points in the solid domain

In figure 3 three different curves are shown. Each of the curves show the temperature behaviour of different points in the solid domain. The three points are centred in between the two interfaces and at different x-positions and show that the solid domain's temperature starts at the initial spatially constant temperature of 300 K. The stationary solution approaches temperatures of around 365 K, 364 K and 362 K, respectively. The simulation results are found to be in a realistic range.

### 4.1 Relaxation method assessment

First, the three different relaxation methods discussed in section 3.5 were investigated. Several simulations were carried out for this purpose. As the MVQN method allows the specification of how many past iterations should be considered to construct the Jacobian matrix, it will be referred to as MVQN $\eta$ in the following, where $\eta$ is the number of past iterations considered. To see the differences induced by the number of past iterations considered, three different values for $\eta$ were chosen.

As can be seen in figure 4, the total number of iterations tends to decrease as the time step size increases. This may seem surprising at first, but on reflection it becomes clear that this is because fewer time steps are needed to reach the end of the simulation. Especially towards the end of the simulation, the time steps often only need a single iteration to converge.

In general, the relaxation method appears to have less influence on the sum of coupling iterations than the time step size itself. Especially with a time step size of $\Delta t = 0.02\,\mathrm{s}$ and excluding the constant relaxation method, the other methods all required a similar total number of coupling iterations for the entire simulation.

Furthermore, it can be observed that the constant relaxation method is the least effective of the three methods, as it results in the highest number of coupling iterations required. This was to be expected. In fact, the constant relaxation method did not converge in a reasonable number of coupling iterations using a time step size of $\Delta t = 0.04\,\mathrm{s}$. This is indicated by the black X's in figure 4.

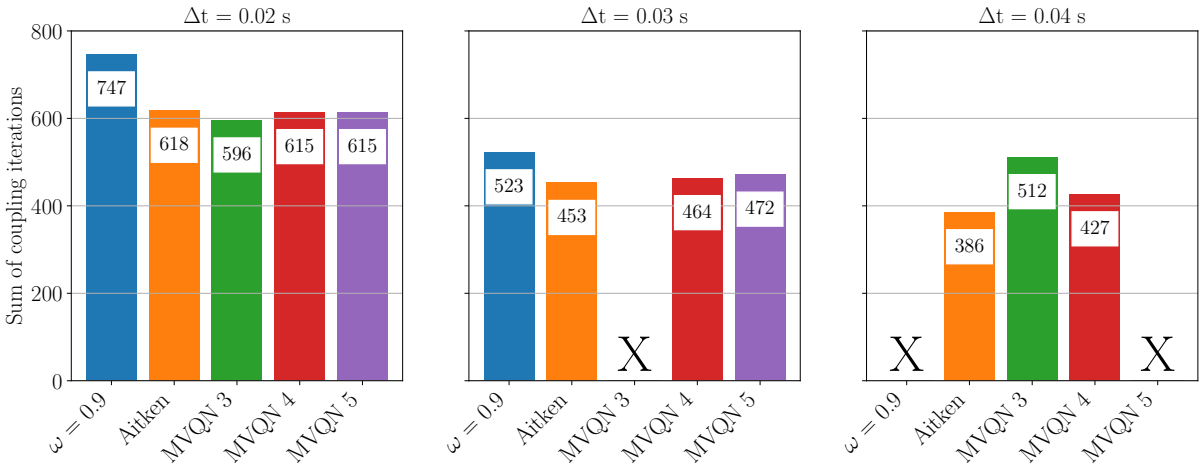


**Figure 4**: Sum of coupling iterations for different relaxation methods

In the simulation with the smallest time step size, the MVQN method shows the best performance considering the last three coupling iterations. However, even with a slightly larger time step, the Aitken method is superior.

In this particular case, the MVQN method appears to require fewer coupling iterations the fewer past iterations are considered. Nevertheless, the MVQN method also appears to be sensitive to its parameter $\eta$. At a time step size of $\Delta t = 0.04\,\mathrm{s}$ this is no longer the case. Here, MVQN 3 required almost as many coupling iterations as the inefficient constant relaxation scheme at a smaller time step size of $\Delta t = 0.03\,\mathrm{s}$.

Overall, it can be observed that the Aitken method shows good performance and excellent stability in the proposed test case. Also in terms of the computational overhead caused by the coupling schemes, the Aitken method shows good performance (see figure 5). Obviously, the computational overhead of the constant relaxation method is the lowest, since no calculations are required at all. For this reason it is not shown in figure 5.

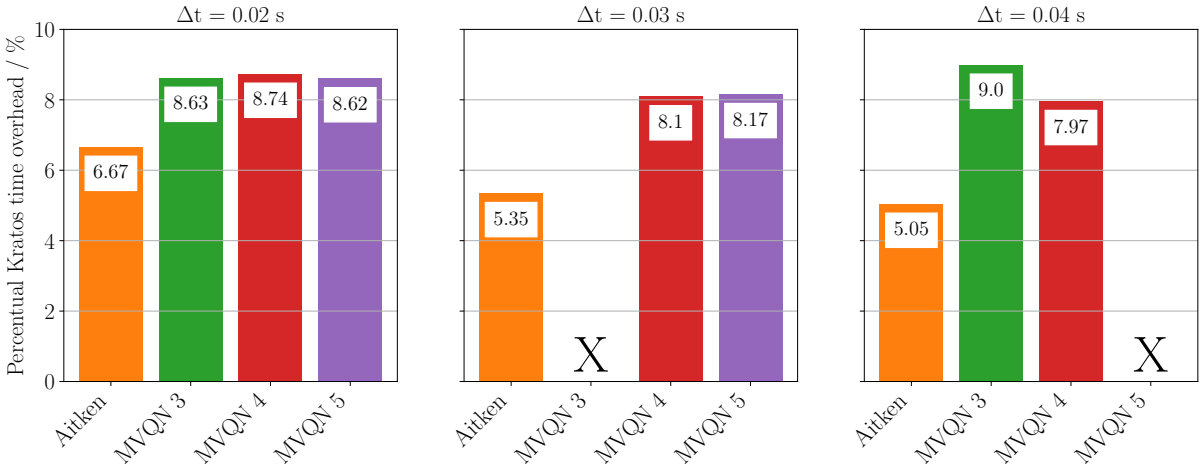


**Figure 5**: Percentual Kratos overhead of simulation time for different relaxation methods

The MVQN scheme shows a similar computational overhead regardless of its parameter $\eta$ and is around 8-9 %. Initially, it also appears that the computational overhead decreases with increasing time step size. However, the simulation with the largest time step size shows an outlier at $\eta = 3$. This is the same simulation that also shows the worst performance in terms of the number of coupling iterations within the simulation with the largest time step size.

### 4.2 Neumann-Dirichlet approach

The difficulties mentioned in section 3.4, which necessitated a pseudo-transient approach, do not apply if at least one Dirichlet boundary condition is imposed to the solid domain. This opens up the possibility of a fully steady-state analysis where all subproblems are considered to be stationary. This type of analysis could dramatically speed up the process.

For this reason, an attempt was made to change the boundary coupling method from an FFTB to a TFFB coupling scheme between the aerodynamic and solid domains. In this case, a temperature boundary condition is applied at the upper solid boundary and the resulting heat

flux is returned to the aerodynamic domain.

As can be seen in figure 6, the temperature rises into extreme regions using this approach. This is because the solid domain returns a high heat flux due to the large temperature gradient between the aerodynamic flow and the initial temperature of the solid domain. As these high heat fluxes are applied to the aerodynamic domain for an infinite time due to its stationarity, the aerodynamic interface temperatures rise to exorbitant levels. Two reasons for this are the low thermal mass of the air, which facilitates the extreme temperature rise, and the low thermal conductivity, which prevents the temperature from being distributed across the aerodynamic domain. Both result in a hot spot just above the coupling interface.

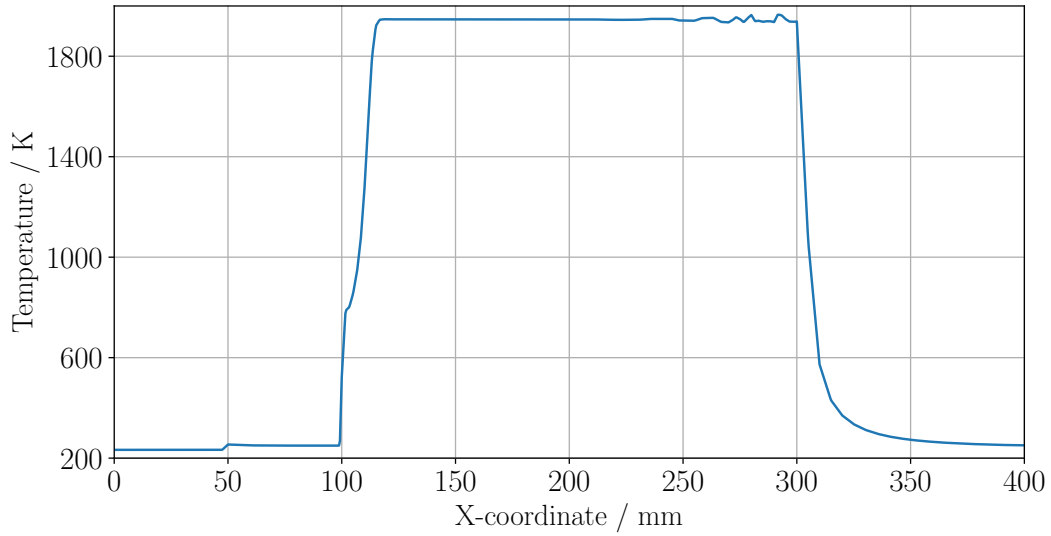


**Figure 6**: Temperatures of the aerodynamic domain at $y = 0$ just before the aerodynamic solver crashes

It is evident that a relaxation factor may be selected in accordance with the objective of achieving convergence in the simulation. However, this relaxation factor would be exceedingly small in comparison to the extent of the heat flux and would also be based on an educated guess. The use of exceedingly small relaxation factors results in an unreasonable number of coupling iterations and is therefore not practical.

## 5 CONCLUSION AND OUTLOOK

In this paper three different coupling relaxation schemes have been applied to a three-field two-dimensional conjugate heat transfer problem. The results show that the Aitken scheme is superior in most simulations. This is due to its good performance in determining an appropriate relaxation factor and its robustness. The MVQN method was sensitive to the number of previous iterations used to construct its Jacobian matrix, sometimes leading to divergence. It was also, in most cases, not as efficient as the Aitken scheme in terms of the number of coupling iterations.

The conventional Dirichlet-Neumann coupling (FFTB) seems to be the only stable method to couple the outer aerodynamics and the solid domain with reasonable relaxation factors. This is due to the low thermal mass and conductivity of the aerodynamic domain. Due to the resulting

very high heat fluxes applied to the aerodynamic domain, the temperature rises excessively and leads to a solver crash.

For further studies, the Aitken scheme is used due to its performance, robustness and low computational cost. It needs to be investigated whether the Neumann-Dirichlet approach (TFFB) shows the same behaviour for other cases, such as 3D flow applications, and what happens when this method is applied to the interface between the solid and cooling fluid domains. Due to the different velocities, densities and viscosities, there are different heat transfer coefficients that could lead to a successful Neumann-Dirichlet coupling. This could be a way of obtaining a Dirichlet boundary condition in each domain, opening up the possibility of a fully steady-state analysis, saving a great deal of computing power.

## ACKNOWLEDGEMENT

The authors would like to acknowledge the funding by the Deutsche Forschungsgemeinschaft (DFG, German Research Foundation) under Germany´s Excellence Strategy – EXC 2163/1 - Sustainable and Energy Efficient Aviation – Project-ID 390881007.

## REFERENCES

[1] Birken, P. et al. “A time-adaptive fluid-structure interaction method for thermal coupling.” Computational and Visualisation in Science (2010) 13:331-340. http://doi.org/10.1007/s00791 -010-0150-4

[2] http://www.openfoam.com/

[3] Küttler, U. and Wall, W. “Fixed-point fluid-structure interaction solvers with dynamic relaxation.” Computational Mechanics (2008) 43:61-72. http://doi.org/10.1007/s00466 -008-0255-5

[4] Bogaers, A.E.J. et al. “Quasi-newton methods for implicit black-box FSI coupling.” Computer Methods in Applied Mechanics and Engineering (2014) 279:113-132. http://doi.org/10.1016/j .cma.2014.06.033

[5] Divo, E. et al. “Glenn-HT/BEM conjugate heat transfer solver for large-scale turbomachinery models.” NASA/CR-2003-212195 (2003). NASA DOC ID 20040000109

[6] Moukalled, F. Mangani, L. and Darwish, M. “The finite volume method in computational fluid dynamics.” Springer Switzerland (2016). http://doi.org/10.1007/978 -3-319-16874-6

[7] http://github.com/KratosMultiphysics/Kratos/tree/master/applications/CoSimulationApplication

[8] VDI e.V. “VDI heat atlas.” Springer Berlin (2010), Heidelberg. http://doi.org/10.1007/978 -3-540-77877-6

[9] Sutherland, W. “The viscosity of gases and molecular force.” The London, Edinburgh, and Dublin Philosophical Magazine and Journal of Science (1893) 36(223):507–531. http://doi.org/10.1080/14786449308620508